

## Variance of the distributions of energy levels and of the transition arrays in atomic spectra. III. Case of spin-orbit-split arrays

C. Bauche-Arnoult and J. Bauche

Laboratoire Aimé Cotton, Centre National de la Recherche Scientifique,  
Bâtiment 505, 91405 Orsay, France

M. Klapisch

Racah Institute of Physics, The Hebrew University, 91904 Jerusalem, Israel

(Received 13 September 1984)

In previous papers formulas for mean wave numbers and spectral widths of transition arrays have been presented. Here the method is extended to the cases  $nl^N n' l_j' - nl^N n'' l_j''$ ,  $(nl_j)^N n' l_j' - (nl_j)^N n'' l_j''$ , and  $(nl_j)^{N+1} - (nl_j)^N n' l_j'$ , i.e., when the spectrum exhibits several subarrays, due to the effects of large spin-orbit interactions. The first case is typical of the x-ray transitions between the internal subshells of the atom. The second and the third cases occur in the vuv and x-ray spectra of highly ionized heavy atoms. The evolution of the array  $3d^8 4s - 3d^8 4p$  along the isoelectronic sequence is presented as a first example of calculation, and criteria for the choice of the relevant formula are proposed. A second example is that of the  $3d^9 - 3d^8 4p$  array in the spectrum of tungsten. Formulas are given (in the Appendices) for the total intensities of subarrays and for the variances of the distribution of energy levels in subconfigurations of the types  $nl^N n' l_j'$  and  $(nl_j)^N (n' l_j')^N$ .

### I. INTRODUCTION

The calculation of the mean value and of the variance of the *wave-number distribution* of the transitions between pure electronic configurations is useful in the interpretation of the spectra of highly ionized atoms. Formulas have been derived<sup>1-3</sup> for these quantities and applications to experimental cases have been presented.<sup>4,5</sup>

Throughout these studies, it has been assumed, or observed experimentally, that the lines of an interconfigurational transition array coalesce into just *one broad band*, whose full width at half maximum (FWHM) and average energy are the significant features. In fact, this is only one extreme situation, where, for instrumental and/or physical reasons, the experimental array is unresolved. Another extreme situation is that in which all the lines can be identified individually. In some intermediate situations the lines of the array are distributed in several bands, whose width may either be small with respect to their separation or of the same order of magnitude.

Two cases are frequently encountered.

(i) The first case is that of the x-ray emission spectra of neutral or weakly ionized atoms. When a vacancy is produced by external means in a closed internal subshell  $n' l'^{4l'+2}$  of the atom, it is soon filled up by an electron of some higher subshell, through radiative transition. If  $l' \neq 0$ , the spin-orbit integral  $\xi_{n'l'} = \int_0^\infty |R_{n'l'}(r)|^2 \xi(r) dr$  is often the largest-energy radial integral in the initial electronic configuration  $n' l'^{4l'+1} n l^N \dots$ , whatever external open subshells  $nl^N \dots$  this configuration may contain. Then, the energies of the initial levels depend primarily on the value of the angular momentum  $j'$  of the internal *hole*  $n' l'^{4l'+1}$  ( $j' = l' \pm \frac{1}{2}$ ), and this leads to split arrays.

(ii) The second case is that of the vuv or x-ray emission

spectra of highly ionized atoms in the hot plasmas of current interest. In such a case the transitions occur within the external subshells of the highly ionized atom. If at least one spin-orbit integral predominates over the electrostatic Slater integrals, the spectrum is split (see, for example, Fig. 3 in Sec. IV).

In both cases it is clear that the variance or FWHM of the *whole* transition array has no physical interest. For example, the  $K\alpha_1$  and  $K\alpha_2$  x-ray lines appear so far apart in the spectrum that it is generally useless to remember that they are, together, the  $2p^{-1} n l^N - 1s^{-1} n l^N$  array (the notation  $nl^{-1}$  representing an  $nl$  vacancy in the closed subshells). The relevant quantities are, now, the average energy and the variance of each of the *subarrays* into which the array splits.

As in the previous studies,<sup>1-3</sup> we can compute the variance of the distribution of the transition wave numbers, weighted by their electric dipole ( $E1$ ) strengths. The results are useful if the other broadening effects are negligible. Such an assumption appears to be valid in the spectra of highly ionized atoms [case (ii) above], but it is not realistic in the x-ray spectra of neutral or weakly ionized atoms [case (i) above], where several other broadening phenomena have a major importance (e.g., see Ref. 6). However, in the latter case the width which we can compute contributes at any rate to the x-ray linewidth.

In the following we are essentially interested in three specific types of subarrays.

(i)  $(nl)^N n' l_j' - (nl)^N n'' l_j''$ , denoted  $l^N j' - l^N j''$  in shortened notation (Sec. II); the complementary subarray,  $l^{4l'+2-N} j'^{-1} - l^{4l'+2-N} j''^{-1}$ , which has the same properties, is typical of the atomic x-ray lines.

(ii)  $(nl_j)^N n' l_j' - (nl_j)^N n'' l_j''$ , denoted  $j^N j' - j^N j''$  (Sec. III B). In Sec. IV we present, as an example, the evolution

of the  ${}_{27}\text{Co}$ -like  $3d^8 4s-3d^8 4p$  subarrays between types  $l^N j'-l^N j''$  and  $j^N j'-j^N j''$  with increasing nuclear charge.

(iii)  $(nl_j)^{N+1}-(nl_j)^N n'l'_j$ , denoted  $j^{N+1}-j^N j'$  (Sec. III C);  $j^{N+1}$  is generally the ground configuration in highly ionized heavy atoms. In Sec. V we show, as an example, the case of the  $3d^9-3d^8 4p$  subarrays.

The above-mentioned examples are comparisons between the formulas developed here for the first and second moments of the distributions of wave numbers and *ab initio* computations of all the lines of the arrays. Keeping the style of the two previous papers of this series, which were purely theoretical, we shall not include here extensive comparisons with experimental data. These, which usually require the present as well as the previously derived formulas, will appear in another series of papers. Nevertheless, we shall very briefly comment, in Sec. VI, on a laser-produced spectrum of highly ionized thulium and see how the new moment formulas allow its interpretation. The formula for the total intensity of a subarray is given in Appendix A and that for the variance of a subconfiguration in Appendix B.

As in Ref. 1, denoted I in the following, the variance is defined as  $\sigma^2 = \mu_2 - (\mu_1)^2$ , where

$$\mu_n = \sum_{a,b} [(b | H | b) - (a | H | a)]^n w_{ab} / W \quad (1)$$

is the  $n$ th moment of the weighted line-wave-number distribution. The weight  $w_{ab}$  of a transition is the  $z$  part of its  $E1$  strength [ $w_{ab} = |(a | Z | b)|^2$ ], and  $W = \sum_{a,b} w_{ab}$ . But, in contradistinction with what was done in I, the sums on  $a$  and  $b$  do not run, respectively, over the complete sets of states of the lower and upper configurations  $A$  and  $B$ , but on subsets defined in the following sections.

As in I, we assume that the configurations of interest are sufficiently isolated for configuration mixing to be negligible. This assumption holds in highly ionized spectra, provided that the extreme situation of Layzer complexes<sup>7</sup> is not reached.

Concerning the average wave number, the quantity of interest is not  $\mu_1$ , but rather

$$\delta E(Y \rightarrow X) = T_{av}(Y \rightarrow X) - [E_{av}(Y) - E_{av}(X)], \quad (2)$$

where  $Y$  and  $X$  are respectively the upper and lower subconfigurations,  $T_{av}(Y \rightarrow X) \equiv \mu_1$ , and  $E_{av}$  is the average wave number of a subconfiguration [in analogy with Eq. (13) in I].

In the sequel each letter  $l, l', l''$  figures unambiguously, either the whole symbol  $nl$ , etc., or only the orbital quantum number  $l$ , etc. Each letter  $j, j'$ , etc., is added as a subscript or even replaces  $nl_j, n'l'_j$ , etc., when  $\xi_{nl}, \xi_{n'l'}$ , etc., is predominant.

## II. SUBARRAYS OF THE $(nl)^N n'l'_j - (nl)^N n''l''_j$ TYPE

In the  $(nl)^N n'l'_j - (nl)^N n''l''_j$  array, denoted  $l^N j' - l^N j''$  in the following, we suppose that  $l'$  and  $l''$  are different from zero and that the spin-orbit integrals  $\xi_{l'}$  and  $\xi_{l''}$  are by far the predominant energy parameters. Each configuration splits in two subconfigurations, characterized by the value  $j' = l' \pm \frac{1}{2}$  or  $j'' = l'' \pm \frac{1}{2}$ . Because of the selection

rules imposed by the electric dipole transition operator  $Z$ ,  $|l'' - l'| = 1$ , and the lines which do not fulfill  $|j'' - j'| \leq 1$  have a negligible strength. Therefore the transition array splits into three subarrays, as shown on Fig. 1 for the case  $l'' = l' + 1$ .

For computing the mean wave number and the variance of each of these subarrays, Eq. (1) can be used, with the summations running over all eigenstates

$$a = |[l^N \Psi'_1, (sl')j'] J' M|, \quad (3)$$

$$b = |[l^N \Psi''_1, (sl'')j''] J'' M|$$

with fixed  $j'$  and  $j''$  values. In Eq. (3) the coupling  $\Psi'_1$  ( $\Psi''_1$ ) depends upon the values of all the energy integrals other than  $\xi_{l'}$  ( $\xi_{l''}$ ).

Apart from these restrictions on the summations, the formal calculation of the variance resembles that of the array  $l^N l' - l^N l''$  in I. In particular, the same products of Slater integrals (PSI) occur as in Table III of I, with the same dependences on  $N$ .

Moreover, the couplings  $\Psi'_1$  and  $\Psi''_1$  in Eq. (3) can generally be chosen in a way appropriate to each desired PSI [among the exceptions are the  $F^k(l, l') G^k(l, l')$  products, for example]. Then, for all PSI, it suffices to calculate the variance by Racah's methods<sup>8</sup> in a simple case ( $N=1$ , or  $4l+1$ ).

The complete expression of the variance  $\sigma^2$  for the subarray  $l^N j' - l^N j''$  is listed in Table I. In this table the

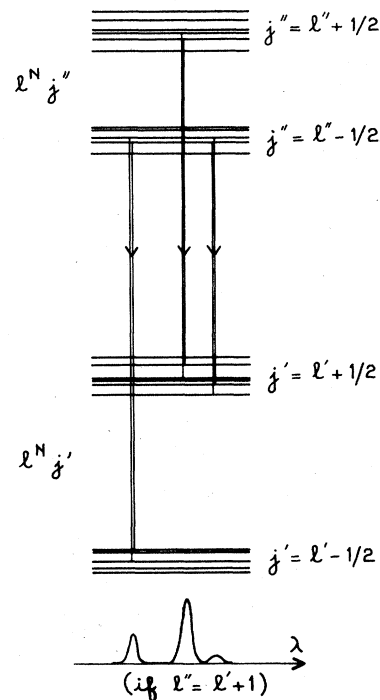


FIG. 1. Splitting of a transition array  $l^N l' - l^N l''$  into subarrays, due to the large values of the spin-orbit integrals of the outer electrons  $l'$  and  $l''$ .

TABLE I. Different parts of the formula giving the variance  $\sigma^2$  of the subarray  $(nl)^N n' l'_j - (nl)^N n'' l''_j$ .  $t = N(4l - N + 2)$ .

---


$$K_2 = \sum_{k \neq 0} \sum_{k' \neq 0} \frac{\delta(k, k')}{2k+1} \left\{ \begin{matrix} j' & k & j' \\ l' & \frac{1}{2} & l' \end{matrix} \right\}^2 \frac{(2j'+1)(2l+1)(2l'+1)^2}{4l+1} \begin{bmatrix} l & k & l \\ 0 & 0 & 0 \end{bmatrix}^2 \begin{bmatrix} l' & k & l' \\ 0 & 0 & 0 \end{bmatrix}^2 t F^k(l') F^{k'}(l').$$

$K'_2$ : Same as  $K_2$  with  $l''$  and  $j''$  replacing  $l'$  and  $j'$ , respectively .

$$K_3 = \sum_k \sum_{k'} \left[ \frac{\delta(k, k')}{2k+1} \frac{(2j'+1)(2l+1)}{2(4l+1)} - \frac{1}{4(4l+1)} \right] \begin{bmatrix} l & k & l' \\ 0 & 0 & 0 \end{bmatrix}^2 \begin{bmatrix} l & k' & l' \\ 0 & 0 & 0 \end{bmatrix}^2 t G^k(l') G^{k'}(l').$$

$K'_3$ : Same as  $K_3$  with  $l''$  and  $j''$  replacing  $l'$  and  $j'$ , respectively .

$$K_4 = \sum_{k \neq 0} \sum_{k'} (-1)^{k'+1} \left\{ \begin{matrix} j' & k & j' \\ l' & \frac{1}{2} & l' \end{matrix} \right\}^2 \begin{bmatrix} l & k & l \\ 0 & 0 & 0 \end{bmatrix} \frac{(2j'+1)(2l+1)(2l'+1)^2}{4l+1} \begin{bmatrix} l & k & l \\ 0 & 0 & 0 \end{bmatrix} \begin{bmatrix} l' & k & l' \\ 0 & 0 & 0 \end{bmatrix} \begin{bmatrix} l & k' & l' \\ 0 & 0 & 0 \end{bmatrix}^2 t F^k(l') G^{k'}(l').$$

$K'_4$ : Same as  $K_4$  with  $l''$  and  $j''$  replacing  $l'$  and  $j'$ , respectively .

$$K_5 = \sum_{k \neq 0} \sum_{k' \neq 0} \frac{-2\delta(k, k')}{2k+1} \left\{ \begin{matrix} j' & k & j' \\ l' & \frac{1}{2} & l' \end{matrix} \right\} \left\{ \begin{matrix} j'' & k & j'' \\ l'' & \frac{1}{2} & l'' \end{matrix} \right\} \left\{ \begin{matrix} j'' & k & j'' \\ j' & 1 & j' \end{matrix} \right\} \frac{(2j'+1)(2j''+1)(2l+1)(2l'+1)(2l''+1)}{4l+1} \\ \times \begin{bmatrix} l & k & l \\ 0 & 0 & 0 \end{bmatrix}^2 \begin{bmatrix} l' & k & l' \\ 0 & 0 & 0 \end{bmatrix} \begin{bmatrix} l'' & k & l'' \\ 0 & 0 & 0 \end{bmatrix} t F^k(l') F^{k'}(l'').$$

$$K_6 = \sum_k \sum_{k'} \left[ \frac{1}{2(4l+1)} - \frac{\left\{ \begin{matrix} k & 1 & k' \\ l'' & l & l' \end{matrix} \right\}^2 \left\{ \begin{matrix} j' & 1 & j'' \\ l'' & \frac{1}{2} & l' \end{matrix} \right\}^2}{4l+1} \frac{(2j'+1)(2j''+1)(2l+1)(2l'+1)(2l''+1)}{4l+1} \right] \\ \times \begin{bmatrix} l & k & l' \\ 0 & 0 & 0 \end{bmatrix}^2 \begin{bmatrix} l & k' & l'' \\ 0 & 0 & 0 \end{bmatrix}^2 t G^k(l') G^{k'}(l'').$$

$$K_7 = \sum_{k \neq 0} \sum_{k'} (-1)^k \left\{ \begin{matrix} j' & k & j' \\ l' & \frac{1}{2} & l' \end{matrix} \right\} \left\{ \begin{matrix} j'' & k & j'' \\ j' & 1 & j' \end{matrix} \right\} \left\{ \begin{matrix} j'' & k & j'' \\ l'' & \frac{1}{2} & l'' \end{matrix} \right\} \begin{bmatrix} l & k & l \\ l'' & k' & l'' \end{bmatrix} \frac{(2j'+1)(2j''+1)(2l+1)(2l'+1)(2l''+1)}{4l+1} \\ \times \begin{bmatrix} l & k & l \\ 0 & 0 & 0 \end{bmatrix} \begin{bmatrix} l' & k & l' \\ 0 & 0 & 0 \end{bmatrix} \begin{bmatrix} l & k' & l'' \\ 0 & 0 & 0 \end{bmatrix}^2 t F^k(l') G^{k'}(l'').$$

$K'_7$ : Same as  $K_7$  with  $l'$  and  $j'$  interchanged with  $l''$  and  $j''$ , respectively .

---

spin-orbit integrals  $\xi_{l'}$  and  $\xi_{l''}$  do not occur, of course, and also not the differences  $\Delta F^k = F^k(l, l)$  (in  $l^N l'$ ) -  $F^k(l, l)$  (in  $l^N l''$ ) and  $\Delta \xi_{nl} = \xi_{nl}$  (in  $l^N l'$ ) -  $\xi_{nl}$  (in  $l^N l''$ ), which are supposed to be equal to zero, for the sake of simplicity. Each line is denoted  $K_i$  or  $K'_i$ , with the subscript  $i$  progressing down Table I in analogy with Table III of I.

For the subarray average wave number, the quantity  $\delta E$  defined in Eq. (2) turns out to be  $\delta E(l^N j' - l^N j'') = 0$ , in analogy with Eq. (12) of I. If a passive open subshell  $\lambda^v$  is added, it can be shown, along the same lines as in Ref. 2, that

$$\sigma^2(\lambda^v l^N j' - \lambda^v l^N j'') = \sigma^2(l^N j' - l^N j'') + \sigma^2(\lambda^v j' - \lambda^v j''). \quad (4)$$

Now, if we suppose that  $l'$ , say, vanishes, results listed in Table I and the above remarks are still valid, because the coupling defined in Eq. (3) can still be written. However, the transition array splits into two subarrays, instead of three like in Fig. 1, because the lower configuration does not split.

### III. SUBARRAYS IN PURE $j$ - $j$ COUPLING

#### A. Principles

It frequently happens, in heavy atomic ions, that all the spin-orbit integrals in the open subshells predominate over the Slater integrals. Then, the coupling is of the  $j$ - $j$  type in both configurations, and the transition array splits into several subarrays. As in I, we have studied the cases  $l^N l' - l^N l''$  and  $l^{N+1} - l^N l'$ .

The example of the  $d^2 p - d^2 d'$  array is displayed in Fig. 2, in the assumption of vanishing Slater integrals. Each configuration splits into six subconfigurations, represented by horizontal segments. Because the ionic core  $d^2$  must not change in the transition, and because of the selection rule  $|j'' - j'| \leq 1$  for the jumping electron, the array splits into nine subarrays only, represented by vertical arrows. The wave-number splittings between these subarrays are such that only three lines can be seen in the spectrum, each one being the superposition of three subarrays. In fact, the splittings between the peaks are equal to

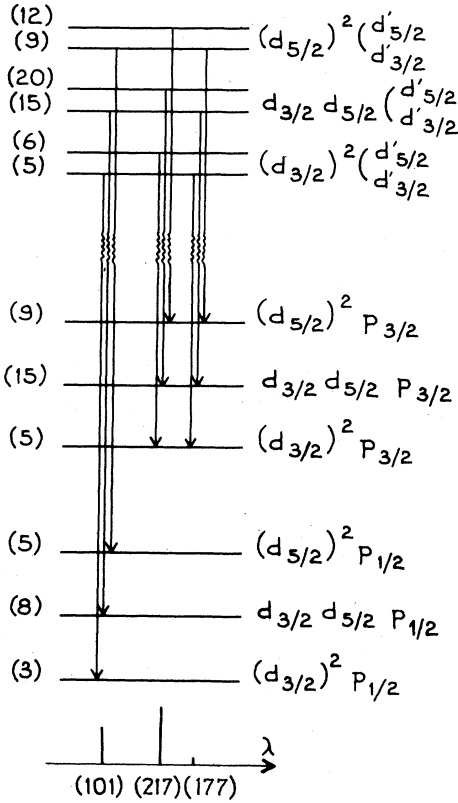


FIG. 2.  $d^2p-d^2d'$  transition array. For the sake of simplicity, the Slater integrals are supposed to be zero. Each configuration splits into six degenerate subconfigurations (degeneracy in brackets). The nine allowed subarrays group into three peaks (number of lines in brackets).

those between the lines of the one-electron  $p-d'$  array. Now, in physical cases the Slater integrals do not vanish; it may only happen that their effect is much smaller than that of the spin-orbit integrals. Thus, the three lines in Fig. 2 are replaced by broad peaks.

The case of the  $l^{N+1}-l^{Nl'}$  arrays in pure  $j-j$  coupling is

TABLE II. Example of the  $d^3-d^2p$  transition subarrays. On the spectrum, only three peaks can be seen, each one resulting from the superposition of three subarrays and corresponding to the transitions  $d_{3/2}-p_{1/2}$ ,  $d_{3/2}-p_{3/2}$ , and  $d_{5/2}-p_{3/2}$ . The right-hand side gives the type of each subarray referring to Secs. III B and III C.

Subarray	Type
$d_{3/2}^3-d_{3/2}^2p_{1/2}$	$j^{N+1}-j^Nj'$
$-d_{3/2}^2p_{3/2}$	$j^{N+1}-j^Nj'$
$d_{3/2}^2d_{5/2}-d_{3/2}d_{5/2}p_{1/2}$	$j^{N+1}-j^Nj'$ (plus spectator $d_{5/2}$ )
$-d_{3/2}d_{5/2}p_{3/2}$	$j^{N+1}-j^Nj'$ (plus spectator $d_{5/2}$ )
$-d_{3/2}^2p_{3/2}$	$j^Nj'-j^Nj''$
$d_{3/2}d_{5/2}^2-d_{3/2}^2p_{1/2}$	$j^Nj'-j^Nj''$
$-d_{5/2}^2p_{3/2}$	$j^Nj'-j^Nj''$
$-d_{3/2}d_{5/2}p_{3/2}$	$j^{N+1}-j^Nj'$ (plus spectator $d_{3/2}$ )
$d_{5/2}^3-d_{5/2}^2p_{3/2}$	$j^{N+1}-j^Nj'$

somewhat more complicated. The example of the  $d^3-d^2p$  array is presented in Table II. Each line refers to one of the subarrays. Only three broad bands appear in the spectrum, corresponding to the three one-electron lines  $d_{3/2}-p_{1/2}$ ,  $d_{3/2}-p_{3/2}$ , and  $d_{5/2}-p_{3/2}$  and resulting from the superposition of subarrays.

In brief, it appears that all the subarrays of the  $l^{Nl'}-l^{Nl''}$  and  $l^{N+1}-l^{Nl'}$  arrays belong to one of the following two classes: (i)  $j^Nj'-j^Nj''$ , with a possible passive  $j''^{N''}$  open subshell in both configurations; (ii)  $j^{N+1}-j^Nj'$ , with a possible passive  $j''^{N''}$  open subshell in both configurations. Each subarray of  $d^3-d^2p$  is assigned a class in the right part of Table II.

B. Subarrays of the  $j^Nj'-j^Nj''$  type

In the application of Eq. (1), the summations now run over all eigenstates

$$a = |[j^N\Psi_1, (s'l')j']J'M\rangle, \tag{5}$$

$$b = |[j^N\Psi_1'', (s'l'')j'']J''M\rangle$$

with fixed  $j, j',$  and  $j''$  values. The principles of the calculations resemble those for  $l^Nj'-l^Nj''$  (Sec. II). The results for the variance are listed in Table III, which is presented in the same general way as Table I.

Three points are noteworthy.

(i) As each of the Slater integrals enters the formula for the variance together with a reduced matrix element of the  $(j_1||C^{(k)}||j_2)$  type, we have chosen to express the latter through the formula

$$((s_1l_1)j_1||C^{(k)}||(s_2l_2)j_2) = (-1)^{j_2+k+1/2} \sqrt{(2j_1+1)(2j_2+1)} \times \begin{pmatrix} j_1 & k & j_2 \\ \frac{1}{2} & 0 & -\frac{1}{2} \end{pmatrix} \tag{6}$$

with the assumption that  $l_1+k+l_2$  is even (see Ref. 9).

(ii) It will be useful in Sec. V to consider the case where  $n'l$  and, say,  $n'l'$  are identical, provided that  $j \neq j'$ . In that case the PSI  $F^k(l,l')F^k(l,l')$ ,  $G^k(l,l')G^k(l,l')$ , and  $F^k(l,l')G^k(l,l')$  are actually identical (but not their angular coefficients in the variance expression, of course).

TABLE III. Different parts of the formula giving the variance  $\sigma^2$  of the subarray  $(nl_j)^N n' l'_j - (nl_j)^N n'' l''_j$ .  $y' = N(N-1)(2j-N)(2j-N+1)$ ,  $t' = N(2j-N+1)$ ,  $\Pi(l, l', k) = [1 + (-1)^{l+l'+k}]/2$ ,  $\Delta F^k = F^k(nl, nl)$  [in  $(nl_j)^N n' l'_j$ ]  $- F^k(nl, nl)$  [in  $(nl_j)^N n'' l''_j$ ].

$$P_1 = \sum_{\substack{k \neq 0 \\ \text{even}}} \sum_{\substack{k' \neq 0 \\ \text{even}}} \left[ \frac{\delta(k, k')}{2k+1} - \frac{1}{2j(2j+1)} + \begin{Bmatrix} j & j & k \\ j & j & k' \end{Bmatrix} \right] \frac{(2j+1)^3}{(2j-2)(2j-1)4j} \begin{Bmatrix} j & k & j \\ \frac{1}{2} & 0 & -\frac{1}{2} \end{Bmatrix}^2 \begin{Bmatrix} j & k' & j \\ \frac{1}{2} & 0 & -\frac{1}{2} \end{Bmatrix}^2 y' \Delta F^k \Delta F^{k'}.$$

$$P_2 = \sum_{\substack{k \neq 0 \\ \text{even}}} \sum_{\substack{k' \neq 0 \\ \text{even}}} \frac{\delta(k, k')}{2k+1} \frac{(2j+1)(2j'+1)}{2j} \begin{Bmatrix} j & k & j \\ \frac{1}{2} & 0 & -\frac{1}{2} \end{Bmatrix}^2 \begin{Bmatrix} j' & k & j' \\ \frac{1}{2} & 0 & -\frac{1}{2} \end{Bmatrix}^2 t' F^k(l'') F^{k'}(l'').$$

$P'_2$ : Same as  $P_2$  with  $l''$  and  $j''$  replacing  $l'$  and  $j'$ , respectively.

$$P_3 = \sum_k \sum_{k'} \left[ \frac{\delta(k, k')}{2k+1} - \frac{1}{(2j+1)(2j'+1)} \right] \frac{(2j+1)(2j'+1)}{2j} \begin{Bmatrix} j & k & j' \\ \frac{1}{2} & 0 & -\frac{1}{2} \end{Bmatrix}^2 \begin{Bmatrix} j & k' & j' \\ \frac{1}{2} & 0 & -\frac{1}{2} \end{Bmatrix}^2 t' \Pi(l, l', k) \Pi(l, l', k') G^k(l'') G^{k'}(l'').$$

$P'_3$ : Same as  $P_3$  with  $l''$  and  $j''$  replacing  $l'$  and  $j'$ , respectively.

$$P_4 = \sum_{\substack{k \neq 0 \\ \text{even}}} \sum_{k'} 2(-1)^{k'} \begin{Bmatrix} j' & j & k' \\ j & j' & k \end{Bmatrix} \frac{(2j+1)(2j'+1)}{2j} \begin{Bmatrix} j & k & j \\ \frac{1}{2} & 0 & -\frac{1}{2} \end{Bmatrix} \begin{Bmatrix} j' & k & j' \\ \frac{1}{2} & 0 & -\frac{1}{2} \end{Bmatrix} \begin{Bmatrix} j & k' & j' \\ \frac{1}{2} & 0 & -\frac{1}{2} \end{Bmatrix}^2 t' \Pi(l, l', k') F^k(l'') G^{k'}(l'').$$

$P'_4$ : Same as  $P_4$  with  $l''$  and  $j''$  replacing  $l'$  and  $j'$ , respectively.

$$P_5 = \sum_{\substack{k \neq 0 \\ \text{even}}} \sum_{\substack{k' \neq 0 \\ \text{even}}} -\frac{2\delta(k, k')}{2k+1} \begin{Bmatrix} j' & j' & k \\ j'' & j'' & 1 \end{Bmatrix} \frac{(2j+1)(2j'+1)(2j''+1)}{2j} \begin{Bmatrix} j & k & j \\ \frac{1}{2} & 0 & -\frac{1}{2} \end{Bmatrix}^2 \begin{Bmatrix} j' & k & j' \\ \frac{1}{2} & 0 & -\frac{1}{2} \end{Bmatrix} \begin{Bmatrix} j'' & k & j'' \\ \frac{1}{2} & 0 & -\frac{1}{2} \end{Bmatrix} t' F^k(l'') F^{k'}(l'').$$

$$P_6 = \sum_k \sum_{k'} \left[ -\begin{Bmatrix} k & k' & 1 \\ j'' & j' & j \end{Bmatrix}^2 + \frac{1}{(2j+1)(2j'+1)(2j''+1)} \right] \frac{2(2j+1)(2j'+1)(2j''+1)}{2j} \\ \times \begin{Bmatrix} j & k & j' \\ \frac{1}{2} & 0 & -\frac{1}{2} \end{Bmatrix}^2 \begin{Bmatrix} j & k' & j'' \\ \frac{1}{2} & 0 & -\frac{1}{2} \end{Bmatrix}^2 t' \Pi(l, l', k) \Pi(l, l'', k') G^k(l'') G^{k'}(l'').$$

$$P_7 = \sum_{\substack{k \neq 0 \\ \text{even}}} \sum_{k'} -(-1)^{k'} \begin{Bmatrix} j'' & j'' & k \\ j' & j' & 1 \end{Bmatrix} \begin{Bmatrix} j'' & j'' & k \\ j & j & k' \end{Bmatrix} \frac{2(2j+1)(2j'+1)(2j''+1)}{2j} \\ \times \begin{Bmatrix} j & k & j \\ \frac{1}{2} & 0 & -\frac{1}{2} \end{Bmatrix} \begin{Bmatrix} j' & k & j' \\ \frac{1}{2} & 0 & -\frac{1}{2} \end{Bmatrix} \begin{Bmatrix} j & k' & j'' \\ \frac{1}{2} & 0 & -\frac{1}{2} \end{Bmatrix}^2 t' \Pi(l, l'', k') F^k(l'') G^{k'}(l'').$$

$P'_7$ : Same as  $P_7$  with  $l'$  and  $j'$  interchanged with  $l''$  and  $j''$ , respectively.

(iii) Table III can also be used if, say,  $l' = 0$ , in which case the array splits into two subarrays only.

Concerning each subarray average wave number, the quantity  $\delta E$  defined in Eq. (2) is zero.

If passive open subshells  $\lambda^v$ ,  $\lambda^{v'}$ , etc., are added, they contribute to  $\sigma^2$  in ways which depend on the magnitudes of the spin-orbit integrals  $\xi_\lambda$ . For example, if  $\xi_\lambda$ ,  $\xi_{\lambda'}$ , etc., are small,

$$\sigma^2(\lambda^v \lambda^{v'} \dots j^N j' - \lambda^v \lambda^{v'} \dots j^N j'') \\ = \sigma^2(j^N j' - j^N j'') + \sigma^2(\lambda^v j' - \lambda^v j'') \\ + \sigma^2(\lambda^{v'} j' - \lambda^{v'} j'') + \dots; \quad (7)$$

if they are all large,

$$\sigma^2(i^v i^{v'} \dots j^N j' - i^v i^{v'} \dots j^N j'') \\ = \sigma^2(j^N j' - j^N j'') + \sigma^2(i^v j' - i^v j'') \\ + \sigma^2(i^{v'} j' - i^{v'} j'') + \dots, \quad (8)$$

with  $i$  ( $i'$ ) being the total angular momentum of a  $\lambda$  ( $\lambda'$ ) electron. It can be noted that Eq. (8), together with Table III, suffices for computing all the subarrays the  $l^N l' - l^N l''$  array splits into, when  $\xi_l$ ,  $\xi_{l'}$ , and  $\xi_{l''}$  are predominant radial integrals.

### C. Subarrays of the $j^{N+1} - j^N j'$ type

In the application of Eq. (1), the summations now run over all eigenvectors

$$a = |j^{N+1} \Psi_1 JM\rangle, \\ b = |[j^N \Psi_1, j'] J'M\rangle \quad (9)$$

with  $j$  and  $j'$  fixed. The results for the variance are listed in Table IV, which is presented in the same general way as Table III [see also (i) and (iii) in Sec. III B].

In the case where each  $F^k(nl, nl)$  Slater integral has the

TABLE IV. Different parts of the formula giving the variance  $\sigma^2$  of the subarray  $(nl_j)^{N+1}-(nl_j)^N n' l'_j$ .  $x'=N(N+1)(2j-N-1)(2j-N)$ ,  $y'=N(N-1)(2j-N)(2j-N+1)$ ,  $z'=N(N-1)(2j-N-1)(2j-N)$ ,  $u'=N(2j-N-1)(2j-N)$ ,  $v'=N(N-1)(2j-N)$ ,  $w'=N(2j-N)$ ,  $F_A^k$  and  $F_B^k$  are the Slater integrals  $F^k(nl, nl)$  in the subconfigurations  $(nl_j)^{N+1}$  and  $(nl_j)^N n' l'_j$ , respectively,  $\Pi(l, l', k) = [1 + (-1)^{l+l'+k}]/2$ .

$$\begin{aligned}
 Q_1 &= \sum_{\substack{k \neq 0 \\ \text{even}}} \sum_{\substack{k' \neq 0 \\ \text{even}}} \left[ \frac{\delta(k, k')}{2k+1} - \frac{1}{2j(2j+1)} + \begin{Bmatrix} j & j & k \\ j & j & k' \end{Bmatrix} \right] \frac{(2j+1)^3}{4j(2j-1)(2j-2)} \\
 &\quad \times \begin{Bmatrix} j & k & j \\ \frac{1}{2} & 0 & -\frac{1}{2} \end{Bmatrix}^2 \begin{Bmatrix} j & k' & j \\ \frac{1}{2} & 0 & -\frac{1}{2} \end{Bmatrix}^2 (x' F_A^k F_A^{k'} + y' F_B^k F_B^{k'} - 2z' F_A^k F_B^{k'}). \\
 Q_2 &= \sum_{\substack{k \neq 0 \\ \text{even}}} \sum_{\substack{k' \neq 0 \\ \text{even}}} \left[ -\frac{\delta(k, k')}{2k+1} \begin{Bmatrix} j & j & k \\ j' & j' & 1 \end{Bmatrix} - \begin{Bmatrix} j & j & k' \\ j & j & k \end{Bmatrix} \begin{Bmatrix} j & j & k' \\ j' & j' & 1 \end{Bmatrix} + \frac{1}{2j(2j+1)} \begin{Bmatrix} j & j & k' \\ j' & j' & 1 \end{Bmatrix} \right] \frac{(2j+1)^3(2j'+1)}{j(2j-1)(2j-2)} \\
 &\quad \times \begin{Bmatrix} j & k & j \\ \frac{1}{2} & 0 & -\frac{1}{2} \end{Bmatrix}^2 \begin{Bmatrix} j & k' & j \\ \frac{1}{2} & 0 & -\frac{1}{2} \end{Bmatrix}^2 \begin{Bmatrix} j' & k' & j' \\ \frac{1}{2} & 0 & -\frac{1}{2} \end{Bmatrix} [u' F_A^k F^{k'}(l'l') + v' F_B^k F^{k'}(l'l')]. \\
 Q_3 &= \sum_{\substack{k \neq 0 \\ \text{even}}} \sum_{\substack{k' \neq 0 \\ \text{even}}} \left[ -\begin{Bmatrix} k & k' & 1 \\ j' & j & j \end{Bmatrix}^2 + \begin{Bmatrix} j' & j' & k \\ j & j & 1 \end{Bmatrix} \begin{Bmatrix} j' & j' & k \\ j & j & k' \end{Bmatrix} - \frac{1}{2j(2j+1)} \left[ \frac{\delta(k', 1)}{3} - \frac{1}{2j'+1} \right] \right] \frac{(2j+1)^3(2j'+1)}{j(2j-1)(2j-2)} \\
 &\quad \times \begin{Bmatrix} j & k & j \\ \frac{1}{2} & 0 & -\frac{1}{2} \end{Bmatrix}^2 \begin{Bmatrix} j & k' & j' \\ \frac{1}{2} & 0 & -\frac{1}{2} \end{Bmatrix}^2 \Pi(l, l', k') [u' F_A^k G^{k'}(l'l') + v' F_B^k G^{k'}(l'l')]. \\
 Q_4 &= \sum_{\substack{k \neq 0 \\ \text{even}}} \sum_{\substack{k' \neq 0 \\ \text{even}}} \left[ \frac{\delta(k, k')}{(2k+1)(2j'+1)} - \begin{Bmatrix} j & j & k \\ j & 1 & j' \end{Bmatrix} - \frac{1}{2j} \begin{Bmatrix} j & j' & 1 \\ j' & j & k \end{Bmatrix} \begin{Bmatrix} j & j' & 1 \\ j' & j & k' \end{Bmatrix} \right] \frac{(2j+1)^2(2j'+1)^2}{2j(2j-1)} \\
 &\quad \times \begin{Bmatrix} j & k & j \\ \frac{1}{2} & 0 & -\frac{1}{2} \end{Bmatrix} \begin{Bmatrix} j' & k & j' \\ \frac{1}{2} & 0 & -\frac{1}{2} \end{Bmatrix} \begin{Bmatrix} j & k' & j \\ \frac{1}{2} & 0 & -\frac{1}{2} \end{Bmatrix} \begin{Bmatrix} j' & k' & j' \\ \frac{1}{2} & 0 & -\frac{1}{2} \end{Bmatrix} w' F^k(l'l') F^{k'}(l'l'). \\
 Q_5 &= \sum_k \sum_{k'} \left[ \frac{\delta(k, k')}{(2k+1)(2j'+1)} - \begin{Bmatrix} j & j' & k \\ j' & 1 & j \end{Bmatrix} - \frac{1}{2j} \left[ \frac{\delta(k, 1)}{3} - \frac{1}{2j'+1} \right] \left[ \frac{\delta(k', 1)}{3} - \frac{1}{2j'+1} \right] \right] \\
 &\quad \times \frac{(2j+1)^2(2j'+1)^2}{2j(2j-1)} \begin{Bmatrix} j & k & j' \\ \frac{1}{2} & 0 & -\frac{1}{2} \end{Bmatrix}^2 \begin{Bmatrix} j & k' & j' \\ \frac{1}{2} & 0 & -\frac{1}{2} \end{Bmatrix}^2 \Pi(l, l', k) \Pi(l, l', k') w' G^k(l'l') G^{k'}(l'l'). \\
 Q_6 &= \sum_{\substack{k \neq 0 \\ \text{even}}} \sum_{k'} \left[ \frac{-1}{2j'+1} \begin{Bmatrix} j' & j' & k \\ j & j & k' \end{Bmatrix} - (-1)^{j+j'} \begin{Bmatrix} k & k' & 1 \\ j & j' & j' \end{Bmatrix} \begin{Bmatrix} k & k' & 1 \\ j' & j & j \end{Bmatrix} + \frac{1}{2j} \begin{Bmatrix} j & j' & 1 \\ j' & j & k \end{Bmatrix} \left[ \frac{\delta(k', 1)}{3} - \frac{1}{2j'+1} \right] \right] \\
 &\quad \times \frac{(2j+1)^2(2j'+1)^2}{j(2j-1)} \begin{Bmatrix} j & k & j \\ \frac{1}{2} & 0 & -\frac{1}{2} \end{Bmatrix} \begin{Bmatrix} j' & k & j' \\ \frac{1}{2} & 0 & -\frac{1}{2} \end{Bmatrix} \begin{Bmatrix} j & k' & j' \\ \frac{1}{2} & 0 & -\frac{1}{2} \end{Bmatrix}^2 \Pi(l, l', k') w' F^k(l'l') G^{k'}(l'l').
 \end{aligned}$$

same value in both subconfigurations, the formulas simplify, as

$$\begin{aligned}
 x' + y' - 2z' &= 4N(2j-N)(j-1), \\
 u' + v' &= 2N(2j-N)(j-1).
 \end{aligned}
 \tag{10}$$

The application of Table IV when  $j = \frac{1}{2}$  can always be avoided.

In the evaluation of the subarray average wave number, the quantity  $\delta E$  defined in Eq. (2) reads

$$\delta E = N \left[ - \sum_{\substack{k \neq 0 \\ \text{even}}} \frac{(2j+1)(2j'+1)}{2j} \begin{Bmatrix} k & j & j \\ 1 & j' & j' \end{Bmatrix} \begin{Bmatrix} j & k & j \\ \frac{1}{2} & 0 & -\frac{1}{2} \end{Bmatrix} \begin{Bmatrix} j' & k & j' \\ \frac{1}{2} & 0 & -\frac{1}{2} \end{Bmatrix} F^k(l'l') \right. \\ \left. + \sum_k \frac{(2j+1)(2j'+1)\delta(k,1)-3}{6j} \begin{Bmatrix} j & k & j' \\ \frac{1}{2} & 0 & -\frac{1}{2} \end{Bmatrix}^2 \pi(l,l',k) G^k(l'l') \right] \quad (11)$$

while the average wave numbers  $E_{av}$  of the subconfigurations can be evaluated by means of the tables published by Larkins.<sup>10</sup>

If passive open subshells  $\lambda^v$ ,  $\lambda^{v'}$ , etc., are added, they contribute to  $\sigma^2$  in ways which depend on the magnitudes of the spin-orbit integrals  $\xi_{\lambda}$ ,  $\xi_{\lambda'}$ , etc. For example, if these integrals are small,

$$\sigma^2(\lambda^v \lambda^{v'} \dots j^{N+1} \lambda^v \lambda^{v'} \dots j^N j') \\ = \sigma^2(j^{N+1} j^N j') + \sigma^2(\lambda^v j - \lambda^{v'} j') \\ + \sigma^2(\lambda^{v'} j - \lambda^v j') + \dots ; \quad (12)$$

if they are large,

$$\sigma^2(i^v i^{v'} \dots j^{N+1} i^v i^{v'} \dots j^N j') \\ = \sigma^2(j^{N+1} j^N j') + \sigma^2(i^v j - i^{v'} j') + \sigma^2(i^{v'} j - i^v j') + \dots \quad (13)$$

#### IV. FIRST EXAMPLE: THE $3d^8 4s-3d^8 4p$ ARRAY

We chose the simple  $3d^8 4s-3d^8 4p$  transition array (although it is usually resolved in the observed spectra) as typical of the evolution of the pattern of a transition array along the isoelectronic sequence.

##### A. Evolution of the pattern

In order to fulfill the basic assumption of isolated configurations, we studied the spectra in the range Kr X—W XLVIII, (i.e., from  $Z=36$  to  $Z=74$ ). If we use the crude assumption that the external  $3d$ ,  $4s$ , and  $4p$  orbitals are hydrogenic with the same effective nuclear charge  $Z^*$  ( $\approx Z-26$ ), (i) the  $(3d, 3d)$ ,  $(3d, 4s)$ , and  $(3d, 4p)$  Slater integrals are proportional to  $Z^*$ ; (ii) the spin-orbit  $\xi_{3d}$  and  $\xi_{4p}$  integrals are proportional to  $(Z^*)^4$ ; and (iii) the ratio  $\xi_{3d}/\xi_{4p}$  is independent of  $Z^*$  and equal to  $\frac{64}{135} = 0.47$  (Ref. 11, p. 123).

It is clear from (i) and (ii) that the spin-orbit integrals become predominant when  $Z$  increases. This is the reason for the splitting of the transition array into two subarrays, corresponding, respectively, to the transitions  $4s_{1/2}-4p_{1/2}$  (longer wavelengths) and  $4s_{1/2}-4p_{3/2}$  (shorter wavelengths). Furthermore, in view of (iii), there exist values of  $Z$  for which the  $\xi_{4p}$  integral predominates over the Slater integrals whereas  $\xi_{3d}$  does not.

We used the relativistic parametric-potential code RELAC (Ref. 12) for computing the wavelengths and the  $E1$  transition strengths of the 401 lines of the array  $3d^8 4s-3d^8 4p$  for  ${}_{36}\text{Kr X}$ ,  ${}_{42}\text{Mo XVI}$ , and  ${}_{59}\text{Pr XXXIII}$ . The relativistic Slater integrals obtained were converted into the usual Slater and spin-orbit radial parameters by means of the

formulas published by Larkins<sup>10</sup> and by Bauche *et al.*<sup>13</sup> The corresponding calculated spectra are presented in Fig. 3. The conclusion is that Table III of I gives a satisfactory interpretation of the spectrum in the case of Kr, and Table I of the present paper in the cases of Mo and Pr.

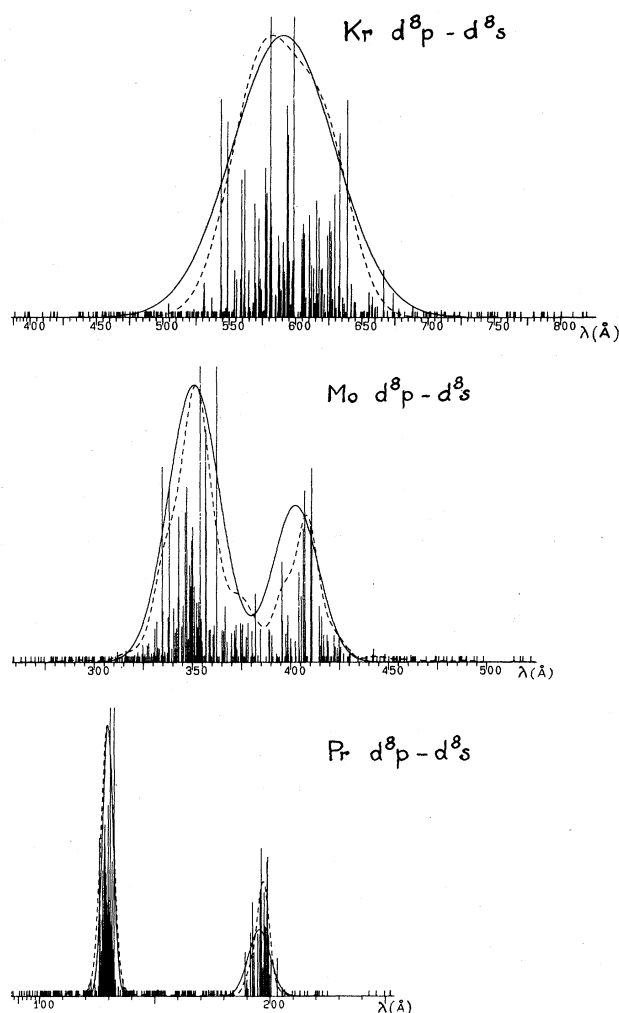


FIG. 3. Examples of calculated spectra in the  $3d^8 4s-3d^8 4p$  series. Each line is represented with a height proportional to its strength, except those with a strength less than 3% of the highest, which have all, conventionally, been increased to that 3% limit. The dashed curves are the envelopes of the line spectra for some small linewidth, sufficient for the coalescence of the lines in one or two peaks. The solid curves are Gaussians whose FWHM have been calculated by means of Table III of I ( ${}_{36}\text{Kr}$ ) and Table I of the present paper ( ${}_{42}\text{Mo}$ ,  ${}_{59}\text{Pr}$ ).

TABLE V. Example of the  $3d^8 4s-3d^8 4p$  series. The full widths at half maximum FWHM1 and FWHM2 have been computed using Table III of I and Table III of the present paper. All entries are in  $\text{cm}^{-1}$ .

	${}_{36}\text{Kr X}$	${}_{42}\text{Mo XVI}$	${}_{48}\text{Cd XXII}$	${}_{54}\text{Xe XXVIII}$	${}_{59}\text{Pr XXXIII}$	${}_{69}\text{Tm XLIII}$	${}_{74}\text{W XLVIII}$
$\Delta_{\text{FWHM}}$ ( $d^8 s-d^8 p$ )	10 579	21 733	42 851	78 691	125 153	283 590	407 195
$\Delta_{\text{FWHM1}}$ ( $d^8 s_{1/2}-d^8 p_{1/2}$ )	11 311	16 071	20 837	25 556	29 428	37 140	41 125
$\Delta_{\text{FWHM2}}$ ( $d^8 s_{1/2}-d^8 p_{3/2}$ )	16 499	24 280	32 212	39 489	45 477	57 478	63 538
$\Delta_{\text{FWHM1}} + \Delta_{\text{FWHM2}}$	27 810	40 351	53 049	65 045	74 905	94 618	104 663
$\frac{3}{2}\zeta_p$	12 870	36 999	83 254	160 825	260 445	598 050	860 790
$\frac{5}{2}\zeta_d$	10 905	27 955	59 170	109 772	174 712	386 415	543 107
$\frac{1}{2}F^2(3d,3d)$	85 748	117 240	148 159	189 519	215 270	265 832	291 697

### B. Choice of the variance formula

First, let us recall that it would be generally incorrect to consider an  $l^{N+1}-l^N l'$  (or  $l^N l'-l^N l''$ ) array as a superposition of subarrays  $j^{N+1}-j^N j'$  (or  $j^N j'-j^N j''$ ). Indeed, doing so would mean neglecting the off-diagonal Hamiltonian matrix elements between the  $jj$  subconfigurations. These are, however, responsible for the departure from pure  $jj$  coupling and are not the predominant integrals. Thus the question of the choice of the proper formula is unavoidable.

Now, we shall propose some simple criteria for choosing the variance formula adapted to the physical case of interest. The first criterion to be found concerns the choice between the cases  $l^N l'-l^N l''$  (one peak) and  $l^N j'-l^N j''$  (several peaks). For the case of  $d^N s-d^N p$  we have found, through numerical studies of various situations, that such a criterion can be built on the comparison between  $3\zeta_{4p}/2$  (the  $4p$  spin-orbit splitting) and the full widths at half maximum of the two subarrays, calculated by means of Table I: if

$$\Delta_{\text{FWHM}}(d^8 s_{1/2}-d^8 p_{1/2}) + \Delta_{\text{FWHM}}(d^8 s_{1/2}-d^8 p_{3/2}) < 3\zeta_{4p}/2, \quad (14)$$

the separation in two subarrays and the values of their FWHM are meaningful (note that, for a Gaussian curve, the FWHM is equal to  $2.355\sigma$ ).

The second criterion relates to the choice between the cases  $l^N j'-l^N j''$  and  $j^N j'-j^N j''$ , which both correspond to two peaks in the present example ( $l'=0$ ) and to three peaks otherwise. Because each peak, in the  $j^N j'-j^N j''$  case, turns out to be the superposition of several subarrays (see Sec. III A), the FWHM of each of the latter cannot be utilized for defining a criterion. Instead, one could look at the purity of the  $j-j$  coupling in the configurations themselves. Thus, the  $l^N j'-l^N j''$  model would be considered as adequate in the  $3d^8 4s-3d^8 4p$  case when

$$\frac{5}{2}\zeta_{3d} \lesssim \frac{1}{2}F^2(3d,3d) < \frac{3}{2}\zeta_{4p} \quad (15)$$

with  $F^2(3d,3d)$  being the largest Slater integral involved. Indeed, the quantities  $\frac{5}{2}\zeta_{3d}$  and  $\frac{3}{2}\zeta_{4p}$  are respectively the

$3d$  and  $4p$  spin-orbit splittings, and the angular coefficients of the  $F^2(3d,3d)$  Slater integral vary by at most one-half inside a  $d^8$  configuration. On the contrary, the  $j^N j'-j^N j''$  model should yield better results when

$$\frac{1}{2}F^2(3d,3d) < \frac{5}{2}\zeta_{3d} < \frac{3}{2}\zeta_{4p}. \quad (16)$$

The numerical results listed in Table V can be used for applying both criteria defined above. First, the comparison between the fourth and fifth lines gives a test of Eq. (14): The conclusion is that the variance of the whole  $3d^8 4s-3d^8 4p$  array is void of physical interest beyond  $Z=45$ . Second, the comparison between the lowest three lines of Table V gives a test of Eqs. (15) and (16): The  $l^N j'-l^N j''$  model should be more adequate for  $Z=50-65$  and  $j^N j'-j^N j''$  beyond  $Z=65$ .

The three ranges of  $Z$  values are clearly visible in Fig. 4, where the curves represent the variations of  $\frac{3}{2}\zeta_p$ ,  $\frac{5}{2}\zeta_d$ ,

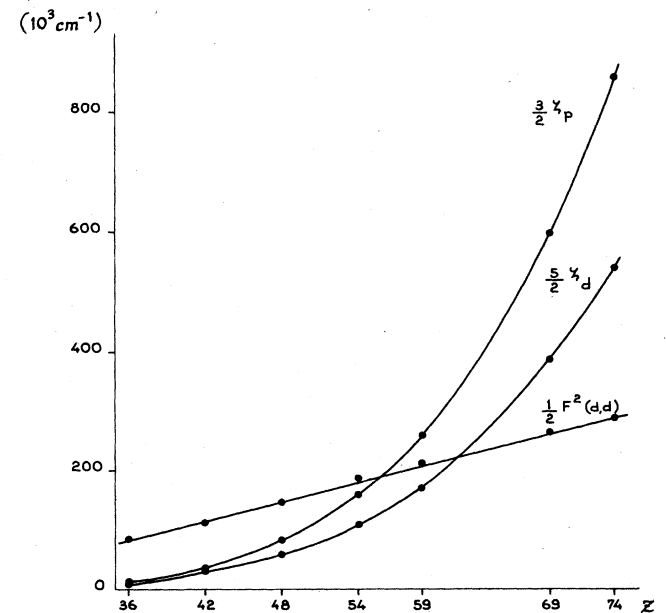


FIG. 4. Values of  $\frac{3}{2}\zeta_p$ ,  $\frac{5}{2}\zeta_d$ , and  $\frac{1}{2}F^2(d,d)$  along the isoelectronic  ${}_{27}\text{Co}$ -like  $3d^8 4s-3d^8 4p$  series.

TABLE VI. Comparison of the FWHM of the two subarrays of the  $d^8s-d^8p$  spectrum, in the cases of  $^{59}\text{Pr XXXIII}$  and  $^{74}\text{W XLVIII}$ . The results given by the two sets of formulas (Tables I and III) can be compared to those of the calculated spectra. All entries are in Å.

		$l^N j' - l^N j''$	$j^N j' - j^N j''$	Calculated spectra
$^{59}\text{Pr XXXIII}$	$d^8s_{1/2} - d^8p_{3/2}$	7.6	5.6	6.9
	$d^8s_{1/2} - d^8p_{1/2}$	11.2	7.7	11.3
$^{74}\text{W XLVIII}$	$d^8s_{1/2} - d^8p_{3/2}$	2.4	1.8	1.9
	$d^8s_{1/2} - d^8p_{1/2}$	6.8	4.6	4.5

and  $\frac{1}{2}F^2(d,d)$  versus  $Z$ . The  $l^N l' - l^N l''$  model is adequate for low  $Z$  values,  $j^N j' - j^N j''$  for large  $Z$  values, and  $l^N j' - l^N j''$  in between. Although the latter range corresponds, strictly speaking, to  $56 < Z < 61$ , we think that  $l^N j' - l^N j''$  is also useful for neighboring values (e.g., for larger  $Z$  values, because it is simpler to apply than the  $j^N j' - j^N j''$  model).

A test of the second criterion can be found in Table VI, where three values of the FWHM of both subarrays of the  $3d^8s-3d^8p$  array are given for the  $^{59}\text{Pr XXXIII}$  and the  $^{74}\text{W XLVIII}$  ions: that calculated in the  $l^N j' - l^N j''$  model (Table I), that in the  $j^N j' - j^N j''$  model (Table III), and that deduced from the subarray envelopes drawn on the spectrum (see Fig. 3). The figures in the third column of Table VI agree better with those of the first one in the  $^{59}\text{Pr}$  case and of the second one in the  $^{74}\text{W}$  case.

Both above criteria can be easily generalized to other types of arrays, especially Eq. (14). For the cases of Eqs. (15) and (16), it can be asserted that  $F^2(nl, nl)$  is the largest relevant Slater integral in  $nl^N n' l'$  configurations.

## V. SECOND EXAMPLE: THE $3d^9-3d^84p$ ARRAY

We chose the  $3d^9-3d^84p$  transition array in the spectrum of  $^{74}\text{W XLVIII}$  ( $_{27}\text{Co}$ -like sequence) as a typical application of the formalism developed in Sec. III. The lines of the array are grouped in three peaks, because both integrals  $\xi_{3d}$  and  $\xi_{4p}$  are large. The calculated spectrum is presented in Fig. 5, namely, the lines computed *ab initio* by means of the RELAC code<sup>12</sup> and three Gaussian curves. Each of these curves represents the superposition of two subarrays: Its mean wave number (variance) is the weighted average of the subarray mean wave number (variance). All the numerical data for the subarrays are listed in Table VII.

The weights of the subarrays can be evaluated in the way described in Appendix A. The most meaningful comparison is that of the Gaussian curves with the envelopes, as in Fig. 3 (see Sec. IV). This comparison is satisfactory.

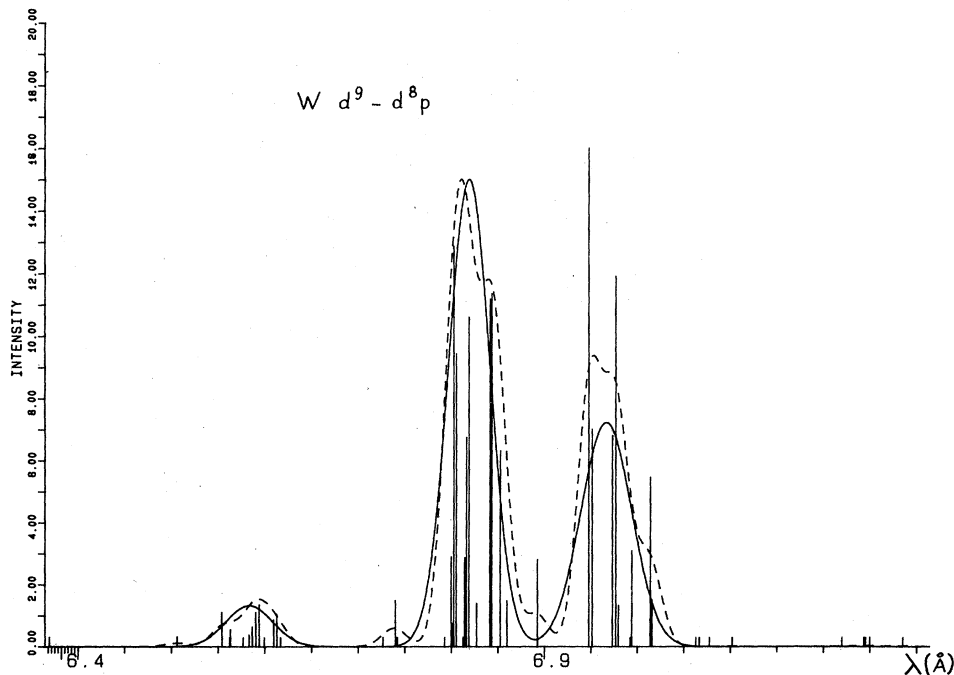


FIG. 5.  $^{74}\text{W XLVIII}$   $3d^9-3d^84p$  transition array. For the definition of the curves, see caption of Fig. 3.

TABLE VII. Details of the calculations of the positions and widths of the different subarrays of the  $3d^9-3d^84p$  transition array in the  ${}_{74}\text{W XLVIII}$  spectrum. ( $d$ ) difference between the mean wave numbers of the subconfigurations. ( $\delta E$ ) shift calculated by means of Eq. (11). (Weight) total strength (see Appendix A). The subarrays 1 and 4, 2 and 5, and 3 and 6 are superposed, and the spectrum exhibits three peaks (see Fig. 5).

Subarrays	No.	$d$ ( $\text{cm}^{-1}$ )	$\delta E$ ( $\text{cm}^{-1}$ )	Axis wave number ( $\text{\AA}$ )	$\sigma$ ( $\text{cm}^{-1}$ )	FWHM ( $\text{\AA}$ )	Weight
$d^3_{3/2}d^6_{5/2}-d^2_{3/2}d^6_{5/2}p_{1/2}$	1	14 342 800	11 324	6.9666	65 625	0.075	5
$-d^2_{3/2}d^6_{5/2}p_{3/2}$	2	15 193 562	-4684	6.5838	67 100	0.068	1
$-d^3_{3/2}d^5_{5/2}p_{3/2}$	3	14 661 202	11 192	6.8155	41 798	0.046	12
$d^4_{3/2}d^3_{5/2}-d^3_{3/2}d^5_{5/2}p_{1/2}$	4	14 337 452	16 986	6.9665	50 858	0.058	10
$-d^3_{3/2}d^5_{5/2}p_{3/2}$	5	15 196 566	-7026	6.5835	52 155	0.053	2
$-d^4_{3/2}d^4_{5/2}p_{3/2}$	6	14 647 942	8954	6.8227	51 905	0.057	15

## VI. CONCLUSION

The  $l^{N+1}-l^Nl'$  and  $l^Nl'-l^Nl''$  arrays are frequently encountered in the spectra of highly ionized atoms. When the spin-orbit interaction is large, they split into subarrays, as was stressed by Cowan.<sup>14</sup> The average wave numbers and the widths of the subarrays  $l^Nj'-l^Nj''$ ,  $j^Nj'-j^Nj''$ , and  $j^{N+1}-j^Nj'$  can be readily calculated by means of the tables and equations above. The influence of passive open subshells, when occurring, is accounted for. Complementary subarrays possess the same properties, in analogy with what is true for the whole arrays.<sup>1,2</sup>

However, many other situations can be considered, among which are the following.

(i) In the  $j^Nj'^{N'+1}-j^{N+1}j'^{N'}$  subarray both relevant subshells are open in both subconfigurations. In analogy with Eq. (8) of Ref. 2, we propose the formulas

$$\sigma^2(j^{N+1}j'^{N'}-j^Nj'^{N'+1}) = \frac{N(2j-N)}{2j-1} \sigma^2(j^2-jj') + \frac{N'(2j'-N')}{2j'-1} \sigma^2(j'^2-jj') \quad (17)$$

for  $j, j' \neq \frac{1}{2}$ , and

$$\delta E(j^Nj'^{N'+1} \rightarrow j^{N+1}j'^{N'}) = \frac{2j'-N'}{2j'} \delta E(j^Nj' \rightarrow j^{N+1}) - \frac{2j-N}{2j} \delta E(j'^{N'}j \rightarrow j'^{N'+1}) \quad (18)$$

(ii) In the  $l^Nl'-l^Nl''$  array it may happen that the only large spin-orbit integral is  $\xi_{l'}$ . We have obtained formulas for the corresponding subarray, denoted  $l^Nj'-l^Nl''$ , which are available upon request.

(iii) The  $l^{N+1}-l^Nj'$  and  $j^{N+1}-j^Nl'$  arrays have not been considered. Actually, we have obtained formulas for the former, which are extremely complicated. The complementary array  $l^{4l-N+1}j'^{2j'+1}-l^{4l-N+2}j'^{2j'}$  could occur, in principle, in x-ray atomic spectra.

(iv) It may happen that the observed subarrays result from the addition of passive open subshells to isolated lines which do not obey  $jj$  coupling (e.g., singlet and trip-

let satellites in  ${}_2\text{He}$ -like ions<sup>15</sup>). In such cases the present formulas cannot be used.

In the same way we have published formulas for the variance of the configurations in I, we give in Appendix B the formulas for the variance of the subconfigurations.

As mentioned earlier, the main purpose of this paper is to develop a formalism, the physical applications of which will be published separately. The case of gold ionized about 50 times is in the course of being published.<sup>16</sup> We present in Fig. 6 the preliminary interpretation of a part of an x-ray spectrum of thulium obtained in laser-produced plasmas. Four  ${}_{28}\text{Ni}$ -like lines have been computed, plus associated satellite subarrays in the  ${}_{29}\text{Cu}$ -

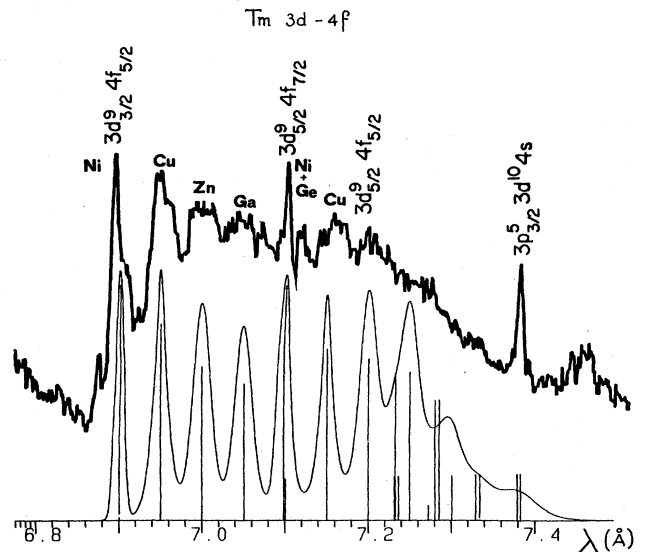


FIG. 6. X-ray spectrum of thulium obtained in a laser-produced plasma. The calculated spectrum consists of Gaussians corresponding to lines of the  ${}_{28}\text{Ni}$ -like spectrum and of associated satellite subarrays in the  ${}_{29}\text{Cu}$ - through  ${}_{32}\text{Ge}$ -like spectra, where spectator electrons are  $4s, 4p, 4d, 4f$ .

through  ${}_{32}\text{Ge}$ -like spectra, with spectator electrons  $4s, 4p, 4d, 4f$ . The overall pattern is fairly well reproduced by the subarray formalism. A more quantitative comparison, requiring a detailed description of the plasma conditions, including optical thickness and intensity scale calibration, is beyond the scope of this paper and will be published elsewhere.

#### APPENDIX A: TOTAL INTENSITIES OF SUBARRAYS

The total strength  $K$  of a subarray can be expressed in terms of the  $E1$  transition radial integral in the nonrelativistic limit

$$I_{nl,n'l'} = \int_0^\infty R_{nl}(r)R_{n'l'}(r)r dr.$$

The basic formula reads

$$K(j^N j'^{N'} \rightarrow j^{N+1} j'^{N'-1}) = l_{>} \begin{Bmatrix} 2j \\ N \end{Bmatrix} \begin{Bmatrix} 2j' \\ N'-1 \end{Bmatrix} \alpha_{ll'jj'} (I_{nl,n'l'})^2, \quad (19)$$

where  $l_{>}$  is the larger of  $l$  and  $l'$ , and where

$$\alpha_{ll'jj'} = (2j+1)(2j'+1) \begin{Bmatrix} j & 1 & j' \\ l' & \frac{1}{2} & l \end{Bmatrix}^2, \quad (20)$$

a quantity symmetrical in  $lj, l'j'$ , whose numerical values are listed in Table VIII. It can be noted that, for each given  $l-l'$  pair in this table, the  $\alpha_{ll'jj'}$  numbers are proportional to the corresponding entries for "SPIN =  $\frac{1}{2}$ " on p. 243 of Ref. 11. The case  $N'=1$  in Eq. (19) gives the answer for the  $j^N j' \rightarrow j^{N+1}$  subarray.

If passive open subshells occur in the subarray, the  $K$  quantity is to be multiplied by their total degeneracy. For example, using Eq. (19) with  $N=0$  and  $N'=1$ , we derive

$$K(l^N j'' \rightarrow l^N j') = l'_{>} \begin{Bmatrix} 4l+2 \\ N \end{Bmatrix} \alpha_{l'l''j'j''} (I_{n'l',n''l''})^2, \quad (21)$$

where  $l'_{>}$  is the larger of  $l'$  and  $l''$ . Numerical examples for the subarrays belonging to the  $d^9-d^8p$  array are listed in the eighth column of Table VII.

The intensity of an emission line is the product of its strength by the fourth power of its wave number, universal constants, and the population of the upper level divided by its degeneracy. Now, the recorded signal depends on the sensitivity of the recorder (e.g., the photographic plate), which is a function of the wave number. Thus, the above strength formulas are useful for the comparison between theory and experiment only in narrow ranges of

TABLE VIII. Calculated values of the factor  $\alpha_{ll'jj'}$  defined in Eq. (19).

Transition	$l$	$j$	$l'$	$j'$	$\alpha_{ll'jj'}$
$s-p$	0	$\frac{1}{2}$	1	$\frac{1}{2}$	$\frac{4}{3}$
	0	$\frac{1}{2}$	1	$\frac{3}{2}$	$\frac{8}{3}$
$p-d$	1	$\frac{1}{2}$	2	$\frac{3}{2}$	$\frac{20}{15}$
	1	$\frac{3}{2}$	2	$\frac{3}{2}$	$\frac{4}{15}$
	1	$\frac{3}{2}$	2	$\frac{5}{2}$	$\frac{36}{15}$
$d-f$	2	$\frac{3}{2}$	3	$\frac{5}{2}$	$\frac{56}{35}$
	2	$\frac{5}{2}$	3	$\frac{5}{2}$	$\frac{4}{35}$
	2	$\frac{5}{2}$	3	$\frac{7}{2}$	$\frac{80}{35}$

wave numbers. Then, the area of a given peak (i.e., the product of its height by its FWHM) is proportional to its calculated total strength multiplied by the average population of the upper states.

For taking into account relativistic corrections in the frame of the Pauli approximation, where the radial functions depend on the  $j$  quantum number, one can replace, in formulas (19) and (21),  $I_{nl,n'l'}$  and  $I_{n'l',n''l''}$  by  $I_{nlj,n'l'j'}$  and  $I_{n'l'j',n''l''j''}$ , respectively.

#### APPENDIX B: VARIANCES OF THE SUBCONFIGURATIONS

The formulas for the variances of the subconfigurations are easily deduced from those for the subarrays, which are listed in Tables I and III:

$$\sigma^2(l^N j') = D_1 + (K_5 + K_6 + K_7), \quad (22)$$

where  $D_1$  can be found in Table I of I, and

$$\sigma^2(j^N j'^{N'}) = P_{1\text{cor}} + P'_{1\text{cor}} + (P_5 + P_6 + P_7)N'(2j' - N' + 1)/2j', \quad (23)$$

where  $P_{1\text{cor}}$  is deduced from  $P_1$  (Table III) by replacing  $\Delta F^k \Delta F^{k'}$  by  $F^k(l,l)F^{k'}(l,l)$ , and  $P'_{1\text{cor}}$  is deduced from  $P_{1\text{cor}}$  by replacing  $N, l, j$  by  $N', l', j'$ .

This straightforward derivation of the subconfiguration variances from the subarray variances can be explained in the same way as, in I, Table I could be deduced from Table III [see the argument under Eq. (11) of I]. It is essentially a consequence of the *J-file sum rule* (Ref. 11, p. 279).

<sup>1</sup>C. Bauche-Arnoult, J. Bauche, and M. Klapisch, Phys. Rev. A **20**, 2424 (1979).

<sup>2</sup>C. Bauche-Arnoult, J. Bauche, and M. Klapisch, Phys. Rev. A **25**, 2641 (1982).

<sup>3</sup>C. Bauche-Arnoult, J. Bauche, and M. Klapisch, J. Opt. Soc.

Am. **68**, 1136 (1978).

<sup>4</sup>M. Klapisch, E. Meroz, P. Mandelbaum, A. Zigler, C. Bauche-Arnoult, and J. Bauche, Phys. Rev. A **25**, 2391 (1982).

<sup>5</sup>M. Klapisch, J. Bauche, and C. Bauche-Arnoult, Phys. Scr. **T3**,

- 222 (1983).
- <sup>6</sup>O. Keski-Rahkonen and M. O. Krause, *At. Data Nucl. Data Tables* **14**, 139 (1974).
- <sup>7</sup>D. Layzer, *Ann. Phys. (N.Y.)* **8**, 271 (1959).
- <sup>8</sup>B. R. Judd, *Operator Techniques in Atomic Spectroscopy* (McGraw-Hill, New York, 1963).
- <sup>9</sup>D. M. Brink and G. R. Satchler, *Angular Momentum* (Clarendon, Oxford, 1968).
- <sup>10</sup>F. P. Larkins, *J. Phys. B* **9**, 37 (1976).
- <sup>11</sup>E. U. Condon and G. Shortley, *The Theory of Atomic Spectra* (Cambridge University, Cambridge, England, 1935).
- <sup>12</sup>E. Luc-Koenig, *Physica (Utrecht)* **62**, 393 (1972); M. Klapisch, *J.-L. Schwob, B. S. Fraenkel, and J. Oreg, J. Opt. Soc. Am.* **67**, 148 (1977).
- <sup>13</sup>J. Bauche, C. Bauche-Arnoult, E. Luc-Koenig, and M. Klapisch, *J. Phys. B* **15**, 2325 (1982).
- <sup>14</sup>R. D. Cowan, *The Theory of Atomic Structure and Spectra* (University of California, Berkeley, 1981), pp. 628 and 629.
- <sup>15</sup>F. Bely-Dubau, J. Dubau, P. Faucher, A. H. Gabriel, M. Loulergue, L. Steenman-Clark, S. Volonté, E. Antonucci, and C. G. Rapley, *Mon. Not. R. Astron. Soc.* **201**, 1155 (1982).
- <sup>16</sup>M. Busquet, D. Pain, J. Bauche, and E. Luc-Koenig, *Phys. Scr.* (to be published).